

We are IntechOpen, the world's leading publisher of Open Access books Built by scientists, for scientists

6,900

Open access books available

186,000

International authors and editors

200M

Downloads

Our authors are among the

154

Countries delivered to

TOP 1%

most cited scientists

12.2%

Contributors from top 500 universities



WEB OF SCIENCE™

Selection of our books indexed in the Book Citation Index
in Web of Science™ Core Collection (BKCI)

Interested in publishing with us?
Contact book.department@intechopen.com

Numbers displayed above are based on latest data collected.
For more information visit www.intechopen.com



Ka-Band HTS System User Uplink SNIR Probability Models

Liping Ai and Hermann J. Helgert

Additional information is available at the end of the chapter

<http://dx.doi.org/10.5772/intechopen.75920>

Abstract

Ka-band High-throughput-satellite (HTS) systems reuse frequency bands in spot beams for much higher system capacity and better spectrum efficiency. They however are prone to intra-system co-color interference and so suffer from the channel signal-to-noise-plus-interference ratio (SNIR) degradation. This chapter presents the development of the uplink SNIR probability models for Ka-band spot beam HTS systems. The models are applicable to different Ka-band propagation channel conditions of statistical significance. Its use of collective representation to model traffic variation of co-color beams captures the statistics of traffic variation and allows feasibility and variety of use case representation. The analytical approach complements known studies and fills in the blank of the use cases of urban and mobile users. The models can be used for system design performance estimation and prediction. It features computation time and memory savings in numerical implementation.

Keywords: spot beam, signal-to-noise-plus-interference ratio (SNIR), probability model, co-color interference (CCI), Ka-band

1. Introduction

Communications satellites have been transitioning from coverage to capacity steadily in the past three decades because of, mainly, the ever increasing demand for high data rates in broadcast and Internet access, and the big data of Internet of Things (IOT). Going higher in spectrum is one way to address the capacity demand. The first dedicated Ka-band experimental advanced communications technology satellite (ACTS) developed and operated by National Astronomy and Space Administration (NASA) concluded the Ka-band precipitation attenuation models and spot beam hopping via on-board switching. Its many experiments laid

out the foundation for the current high throughput satellite (HTS) systems; most of them operate in Ka-band.

A HTS system is a user spot beam system with frequency and polarization (color) reuse applied among spot beams [1]. The higher frequency bands and color reuse increase system capacity or throughput measured by data rate drastically compared to that of the traditional broad beam systems in lower frequency bands without color reuse. Depending on the service area, served population and service type, the later also increase the spectrum efficiency many times. The highest capacity Ka-band HTS system today is ViaSat2 which offers a system throughput of over 270 Gbps.

A variety of uncertainties exist in the complex Ka-band HTS systems including signal propagation channel conditions from a user terminal to satellite, the channel noise, and the varying co-color interference (CCI) power levels. The uncertainties also differ under different system architectures or configurations [2]. They affect the system performance and are studied using probability and statistics before a complex HTS system is constructed. These studies are aimed at assessing system quality of service (QoS) performance matrix against the design specifications and are only feasible via simulations or numerical implementations for a complex system.

The current HTS systems are dominantly geostationary systems for its many advantages [2]. The distinct disadvantage of a HTS system is its many co-color interferers (CCIs) resulted from the color reuse. Moreover, Ka-band systems suffer much higher precipitation attenuation and noise at higher operating frequency bands. Before DVB-S2, site diversity and power control were the only regularly used fade mitigation methods; link availability at 99.9% is very expensive next to unaffordable. With the use of DVB-S2 capable of covering a link budget gap of more than 15 dB and other digital fade mitigation techniques, uninterrupted operation today has become affordable. To select the right combinations of the available digital technologies, the system designers first estimate the system offered signal-to-noise-plus-interference ratio (SNIR) in a system design as part of the estimation of the other system parameters in simulations or numerical implementations of analytical studies at the early stage of a system design.

The SNIR is the fundamental QoS parameter of a communications system [3]. It determines the achievable capacity with known resources and its complementary cumulative distribution leads to link availability directly. In a HTS system, it varies randomly because of the uncertainties of the signal channel, the CCI channels, the uncertain traffic patterns of the CCIs and the random varying noise in the signal channel for a given system layout and a given satellite antenna design. The SNIR variations also defer in different operational scenarios and application types. Therefore to study the user uplink SNIR of an individual channel or a beam average in a HTS system, we first define the operational scenarios within which the SNIR applies. Each application scenario is often also called use case.

In the remainder of this chapter, we start with a discussion of the major prior works known and relevant to our study in Section 2, follow up with system assumptions in Section 3 with a touch of the use cases and proceed to present the user uplink SNIR probability model in Section 4 applying probability theory to the Ka-band slant path channel to satellite together with the collective representation. Then in Section 5, two specific use cases are explored to

show the applications of the SNIR models. Proceeding to Section 6, sample SNIR numerical implementation results of the model system described in Section 3 are evaluated. Finally we conclude our study of the SNIR models and the sample applications in Section 7.

2. Relevant prior work

Several publications reported the research in SNIR estimation for system capacity prediction with iterative and interactive design of the physical layer and the system parameters for a given HTS system with intra-system CCI. In reports by European Space Agency (ESA), a comprehensive HTS system level simulation was described with a model system of 43 spot beams covering Europe and each of the 43 beams is uniformly populated with users [4–7]. The traffic patterns are proportioned and classified for different traffic types with typical traffic probability models. The traffic is fed to each user in a beam one at a time according to the traffic models which is modulated and transmitted to satellite uplink with real system parameters (transmitter EIRP, receiver antenna G/T and etc.). The system adopts multi-frequency time division multiple access (MF-TDMA) system access scheme where a user chooses the channel with the highest power for its traffic delivery which renders one CCI per co-color beam. Typical Ka-band satellite antenna radiation patterns in closed analytical formulas are used for co-color transmission power and signal-to-interference ratio (SIR) distribution estimation. The channel attenuations are assumed fixed. The simulations measure the CCI, SIR, bit-error-rate, call drop rate, link data rates and system capacity at varied system design parameters and traffic load conditions. Two CCI distributions measured at the satellite receiver point are reported in the study, one with the signal beam at the edge of the service coverage area and the other in the center of the service coverage area. The CCI distribution under loaded system condition is symmetric for center located signal beam, resembling a non-central chi-squared (χ^2) probability density function (pdf). It is skewed for the edge located signal beam. The SNIR is not simulated but bench mark calculated.

In another representative HTS system level study, beam average capacity is estimated with the physical layer resource utilization optimization in a loaded system with varied system parameters including transmission powers and reuse size [8]. The system optimization and performance assessment simulation uses the parameters (transmitter EIRP, receiver antenna G/T and etc.). The goal of the study is to improve beam average capacity via DVB-S2X physical layer specification. The total CCI seen by the satellite receiver is simply assumed half-Gaussian distributed in their resource allocation optimization formulated as a mathematical min max problem. The study also reports CCI in χ^2 distribution for the MF-TDMA use case in their Menlo Carlo simulations.

When these studies were made, user uplink traffic is predominately short calls such as web browsing requests, satellite news gathering and email messages. The co-color user powers received by the geostationary satellite are treated as constants in clear-sky (CS) line-of-sight (LOS) channel conditions [4–6, 8]. However, with the introduction of ever increasing number of different data types and operational scenarios such as urban mobile users holding steady

calls, the channel multipath variations are to be included which requires the probability representations of the satellite received powers as well as a collective representation of the total CCI power variation as will be shown later. Our study addresses these use cases.

3. System assumptions

A HTS system typically assumes a system architecture shown in **Figure 1**. It consists of a geostationary satellite relaying the communications traffic in the sky, typically several to about ten gateways and tens of thousands to several hundreds of thousands of users served by the spot beams.

A four co-color reuse with user beams on the right hand side is shown in the figure where total bandwidth for user spots is divided into four sub-bands and each is used by a spot beam marked in one of the four numbers. Every four spot beams numbered one through four form a cluster. The total bandwidth is reused by clusters. The advantage of capacity increase and disadvantage of the intra-system CCI of the HTS system can be deduced from the figure readily. The CCI results because the real antenna radiation patterns do not cease beyond the 3 or 4 dB defined beam edge. In theory, the spots are hexagons seamlessly attach each other or circles with triple cross points for every three adjacent spots as shown in the figure. The circles mark the 3 or 4 dB edge of the spots down from the power of the centers of the spots. In real systems, the spots trace ellipsis contours of different sizes with each contour line indicating a power level. Two channels are defined for the typical digital broadcast and Internet access applications. By DVB-S2 convention, the forward channel is from a gateway via satellite to a user while a reverse channel is from a user via satellite to a gateway. Although Ka-band tropospheric precipitation brings much higher attenuation to the slant path signals, the shorter wavelengths of Ka-band have also made high EIRP directional antenna possible with the

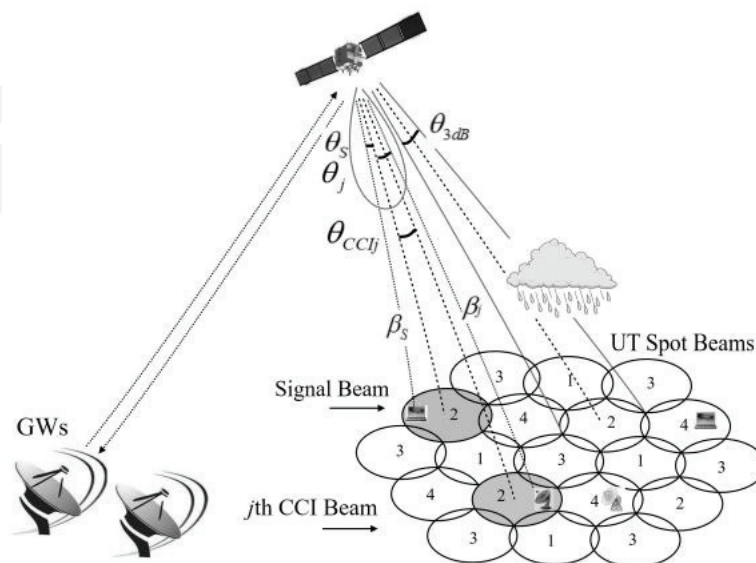


Figure 1. HTS system architecture.

satellite and the gateways. Because gateways typically operate in different frequency bands from that of users and the sites for gateways can be arranged carefully and in advance, interference among gateways uplink is not a performance limiting factor. Our study focuses on the uplink of the reverse channel with users where the color reuse interferences among the spot beams limit the system performance. For its many advantages with geostationary satellite systems, multi-frequency time-division-multiple-access (MF-TDMA) is selected for the model system and it renders one interferer per co-color beam.

The HTS model system which will be used for the system SNIR distribution numerical estimation in this study is a Ka-band system covering US and parts of its borders with 101 spot beams and frequency reuse three as shown in **Figure 2**. The user uplink operates in 30 GHz band. The elliptic spots in the system are in average 350–470 km in minor when illuminated by the geostationary satellite at 99° west with the ITU simple Ka-band satellite antenna radiation pattern at 3 dB apertures of 0.5° side-to-side [9]. The centers of the spot beams are selected a priori according to the service coverage sub-areas. We also assume that there are 1000 users per co-color beam. Each user uses the same user station directional antenna. The user uplink signal received by the satellite is interfered by CCIs because of the imperfect satellite antenna radiation pattern.

The majority of the user reverse channel traffic on the right of **Figure 1** consists of short burst transmissions including emails, network access requests or sales transactions for the second generation Ka-band HTS system applications [10]. This scenario has been studied by simulations and numerical evaluations [4–8]. In this use case, the assumption that the satellite received powers from co-color user transmissions are constants is justified because the signal and CCI power levels vary little in short time frames. Two current application scenarios arise, however, with user reverse channels that require steady transmissions. They are real-time

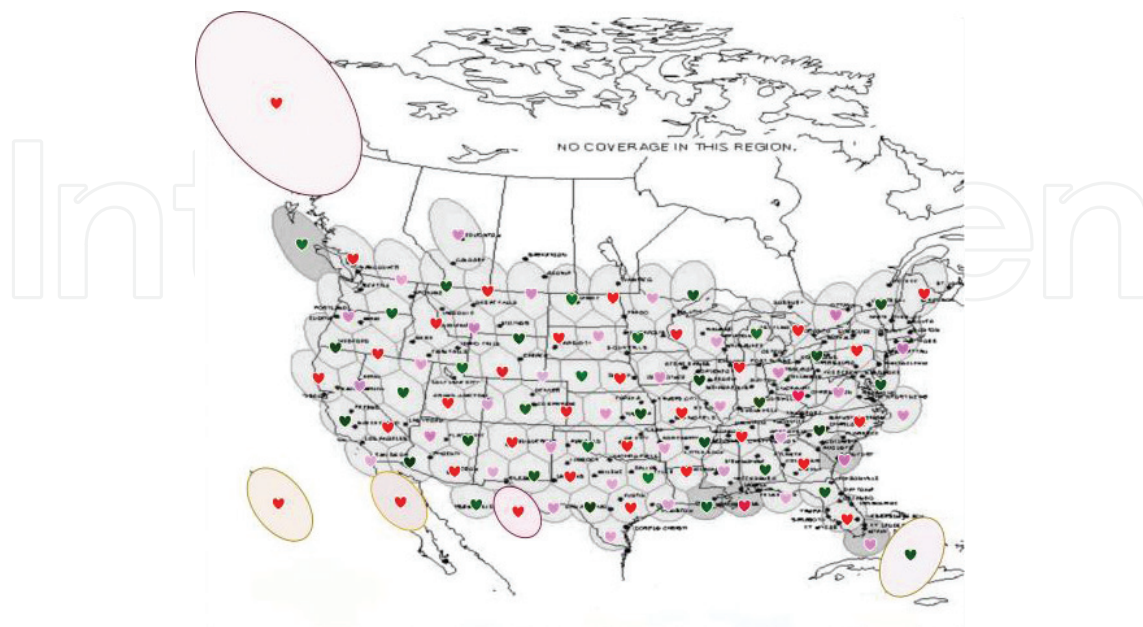


Figure 2. A user spot beam model system.

news gathering return channel defined in DVB-S2 and teleconferencing. Same applies to future systems with Internet-of-Things (IOT) applications such as WiGRID data. All involve multi-path channels typically.

Because of the urban multi-path environments of the links for the two scenarios, the signal and/or co-color interferers' power levels received by satellite antennas vary over time and in space. Therefore they must be treated as random variables [10]. We investigate the two scenarios as one use case and assess its SNIR performance with an analytical approach which results in simple numerical implementation and statistical accuracy.

Figure 3 illustrates the HTS user reverse channel model with major channel impairments of statistical significance [10]. The SNIR is measured at the reference point of the receiver shown in **Figure 3(b)** in this study.

4. User reverse channel SNIR probability model

With reference to **Figure 1** and **3**, we can formulate the user reverse uplink SNIR as:

$$SNIR = \frac{\beta_s \epsilon_s(\alpha_s) G_s(\theta_s)}{N + \sum_{j=1}^n \epsilon_j(\alpha_j) G_j(\theta_j) \beta_j \mu_j} \tag{1}$$

where the Greek symbols can be read by **Figure 1** except ϵ_j , α_j , N and μ_j . We let μ_j be the traffic factor taking a value between 0 and 1 for the fraction of the time of the interferer traffic presence while the signal is in steady transmission, N the channel noise measured at the reference point of **Figure 3(b)** and $\epsilon_j(\alpha_j)$ the user reverse channel transmitter gain in the direction to satellite away from its nadir. It is clear from **Figure 1** that $\epsilon_j(\alpha_j)\beta_j$ is the satellite antenna received signal power while $G_j(\theta_j)$ is the satellite receiver antenna radiation pattern gain in the direction of incoming signal or interferer. The summation term represents the total co-color interference.

Assume that the user terminal antenna radiation patterns are low in EIRP because of their limited sizes, then $\epsilon(\alpha)$ s vary little and Eq. (1) can be simplified to

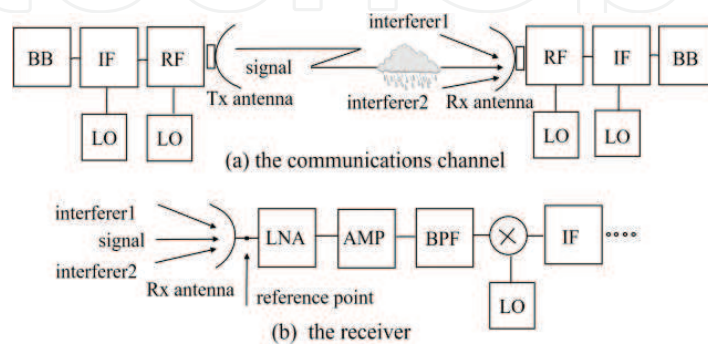


Figure 3. The HTS system uplink transceiver and communications channel.

$$\text{SNIR} = \frac{\beta_s(G)G_s(\theta_s)}{N + \sum_{j=1}^n G_j(\theta_j)(G)\beta_j\mu_j} \quad (2)$$

and further simplified to [10]

$$\text{SNIR} = \frac{\beta_s G_s(\theta_s)}{N + \sum_{j=1}^n \tau_j \beta_j} \quad (3a)$$

$$= \frac{\beta_s G_s(\theta_s)}{N + \tau \tau_0 a \sum_{j=1}^n \beta_j} \quad (3b)$$

by lumping the interferer traffic factors and gains and relocate them outside of the summation. We let τ to represent the traffic factors μ_j collectively while τ_0 satellite antenna angular filtering of the CCIs $G_j(\theta_j)$ collectively. For a mobile user in the urban or open space environment or a stationary user in the urban environment, the user reverse link transmission power varies over time because of the existence of multi-paths. The Rice distribution has long been used for such a propagation channel [10, 11]. It is well known that the Rican distribution is non-central chi-squared (χ^2) distributed in power which can be readily used for the random variable β in clear-sky (CS) line-of-sight (LOS) channel conditions. This χ^2 channel model is applicable for steady transmissions over time in multi-path channel conditions such as urban and mobile users' reverse channels including the future mobile users in autonomous vehicles. It has been shown that the power of SNIR as a random variable in Eq. (3) has a probability density function (pdf) in closed analytical form [10]:

$$f(z)_{S/(den)} = \int_0^\infty y f_{\text{Signal}}(yz) f_{\text{den}}(y) dy \quad (4)$$

where

$$f_{\text{den}} = f_{I_{\text{cllr}}+N} = \left(\int_0^\infty f_I\left(\frac{x}{y}\right) f_{\text{cllr}}(y) \left|\frac{1}{y}\right| dy \right) * f_N \quad (5)$$

is the pdf of the sum of noise random variable and the total CCI random variable. The later has a pdf

$$f_I = f_{\chi^2}(y_{cs}) = \left(\frac{1}{2}\right) e^{-(y_{cs}+\lambda)/2} \left(\frac{y_{cs}}{\lambda}\right)^{\left(\frac{n_1}{2}-\frac{1}{2}\right)} I_{n_1-1}(\sqrt{\lambda y_{cs}}) \quad (6)$$

where * in Eq. (5) denotes convolution; $\lambda = \sum_{i=1}^{n_1} \lambda_i$, λ_i denotes each interferer's χ^2 distribution parameter for CS LOS channels and steady CCI transmission [10, 12]. For the burst short transmission in the same CS LOS channel, constant power received at the satellite can be assumed [4–8, 10]. In this scenario, the CCI pdf in Eq. (5) can be represented by a delta function

$$f_I = \delta(x - I_t) \quad (7)$$

where I_t is the CCI power of short calls received by the satellite receiver, and

$$f_N(x) = n_0 e^{-n_0 x} \quad (8)$$

is the power pdf of the additive-white-Gaussian-noise (AWGN) with noise power density measured at the reference point of **Figure 3** [3, 10].

The pdf f_{cllr} denotes the collective representation of τ and τ_0 in Eq. (3b) as a scaled probability density function to model the satellite received CCI power variations in the user reverse channels. This is possible because the total CCI power seen by the satellite is typically much less than that of the signal. The collective representation will be shown to produce fairly accurate descriptions of typical system operational scenarios. The separation of the nominal CCI power levels and their channel conditions also facilitates the total CCI power pdf representation owing to channel conditions as a single valid pdf shown in Eq. (6) and Eqs. (8–12) [10].

Precipitation is another important channel condition for Ka-band [10, 13]. For a signal and n_2 CCI channels of precipitation, we find the signal power pdf as the function of the rain attenuation model developed by ITU for individual channels [10, 13].

$$f_s(x) = f_{LN}(10(\log(x))) \left(\frac{10}{\ln(10)} \right) \left(\frac{1}{x} \right) \quad (9a)$$

$$= f_{LN}(A_{ps}) \left(\frac{10}{\ln(10)} \right) \left(10^{A_{ps}/10} \right) \quad (9b)$$

where A_p is the ITU rain attenuation random variable in dB. The ITU model predicts annual rain attenuation in dB as lognormal distribution. We then use moment function and Gaussian-Hermit transformation to find the pdf of the sum of n_2 CCI power random variables by equating the means and variances of the lognormal distributions [3, 10, 12]. They give us the total power pdf of n_2 CCI through precipitation slant paths

$$f_I(x) = f_{LN}(10(\log(x))) \left(\frac{10}{\ln(10)} \right) \left(\frac{1}{x} \right) \quad (10a)$$

$$= f_{LN}(A_{pII}) \left(\frac{10}{\ln(10)} \right) \left(10^{A_{pII}/10} \right) \quad (10b)$$

by equating the moment generating functions and applying the Gaussian Hermit transformation:

$$(-1)^{n_2} \prod_{j=1}^{n_2} \left(\sum_{n=1}^k \left(\frac{w_n}{\zeta \sqrt{\tau}} \right) e^{-sI_j(a_n)} \right) = - \sum_{n=1}^k \left(\frac{w_n}{\zeta \sqrt{\tau}} \right) e^{-sI(a_n)} \quad (11)$$

where

$$I_j(a_n) = b \left(10^{-A_{pj}/10} \right) = b \left(10^{-\exp \left(\frac{(\sqrt{2} a_n \sigma_j + \mu_j)}{\zeta} \right) / 10} \right) \quad j = 1, 2, \dots, n_2 \quad (12)$$

$$I(a_n) = n_2 b \left(10^{-A_p/10} \right) = n_2 b \left(10^{-\exp \left(\frac{(\sqrt{2} a_n \sigma + \mu)}{\zeta} \right) / 10} \right) \quad (13)$$

where the (σ_j, μ_j) are known. The (σ, μ) in Eq. (13) can be solved by setting two real values for parameter s in Eqs. (10b–11) [10, 13]. The pair is the lognormal distribution parameters for A_{ptl} in Eq. (10b). The justification for the model selection and development can be found in [10].

5. Collective representation

A quick examination of Eq.(5) shows that the user reverse channel SNIR model consists of noise probability model, the signal and CCI channel models and the collective representation f_{cltr} of the distribution of the total CCI power filtered by traffic activity and the satellite antenna radiation pattern. For all co-color users in multi-path urban or mobile channel conditions of Eq. (6) or Eqs. (8–12), a Beta collective representation in Eq. (3b) represents well the typical 24 h traffic pattern classification of full, heavy, average or light loads for the simplified random user spatial distribution scenarios because all CCI call holding time fall into interval between zero and one when normalized with respect to the signal call holding time [10]. The constant one assumed by the collective traffic τ represents the fully loaded CCI condition. The Beta distribution has a pdf:

$$f_{Bt}(x) = \frac{x^{\alpha-1}(1-x)^{\beta-1}}{B(\alpha, \beta)} \quad (14)$$

Figure 4 shows a typical traffic pattern set in Beta collective representation for the simplified user spatial distribution use case [10]. Let the simplified user location distribution scenario or use case described above is use case one, then the total CCI power filtered by the satellite antenna radiation pattern in Eq. (3b) is represented collectively by a Beta probability distribution function for use case one [10]. In general, depending on the application scenario or use case, it is collectively represented by a combination of probability distribution functions. This is shown later in this section with fully loaded systems of use cases two and three.

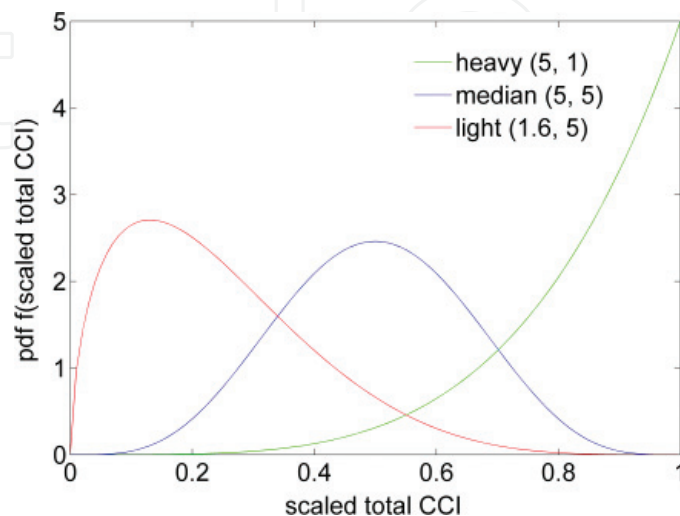


Figure 4. CCI traffic Beta collective representation.

The user reverse channel calls in current HTS systems are most often short calls such as emails or network access requests originated from the randomly located stationary users with CS LOS channels in the co-color beams. In such calling environment, the signal power loss along the slant path to satellite varies little and a constant loss is justified. Another typical use case scenario would be a few urban long holding time calls in the midst of the short stationary calls during the peak hours in the co-color beams of the model system of **Figure 2**. The long calls could be video teleconference calls from an office of an organization header quartered in the downtown area of a city with satellite offices in difference cities of similar urban environments or a news gathering van in an urban area reporting an event during peak traffic hours when the system is loaded. By adaptively applying the models in Section 3 to these two typical use cases, namely, the all short calls use case two and the mixed calls use case three in the model system of **Figure 2** with several further assumptions, we investigate the scenario collective representation in CS LOS channel conditions. First, we expand our original simplified user location assumption to 1000 users uniform or/and Gaussian randomly located in the co-color spot beams. Second, the system is assumed fully loaded. One co-color call at a time from one of the 1000 random user locations is made to the satellite continuously from all co-color beams. This equates the CCI traffic factor in Eq. (3b) to 1 and puts the variation of the total CCI power across the co-color beams received by satellite at the receiver reference point of **Figure 3** dependent on the satellite antenna radiation pattern angular filtering of the incoming CCIs. Finally, the second green beam in the right most column green beams at the edge of the service coverage area in **Figure 2** is designated as the east signal beam (ESB). The rest 32 green beams constitute CCIs to the ESB signal at the satellite receiver. Together, the green 3 reuse system is denoted as ESBg3.

In use case two of all short calls for ESBg3, the total CCI power distribution over time is obtained by summing the 32 CCI gains seen by the satellite antenna at any time instance over equally weighted 1000 time intervals. This distribution at uniform user location distribution can be collectively modeled as a linear combination of two scaled Beta distributions of different parameters:

$$f_{ccis} = f_{cllr} = a_1 f_{Beta1} + b_1 f_{Beta2} \quad (15)$$

For the same system but mixed call use case three, it is a combination of an exponential and a Gaussian distribution:

$$f_{ccis} = f_{cllr} = a_2 f_{exp} + b_2 f_{norm} \quad (16)$$

The parameters $a_1, b_1, a_2, b_2, \lambda$ of f_{exp} , (μ, σ) of f_{norm} , (α_1, β_1) of f_{Beta1} and (α_2, β_2) of f_{Beta2} vary with the type of user location distribution, the satellite antenna radiation pattern and the number of interferers. Clearly, the a s, and b s are constrained by $a + b = 1$. **Figures 5** and **6** show two use cases ESBg3 typical short call CCI power distributions and their collective representations by Eqs. (15–16). The collective approximation can be refined with additional or/and different combinations. The parameters for the two figures are tabulated in **Table 1** of Appendix A.

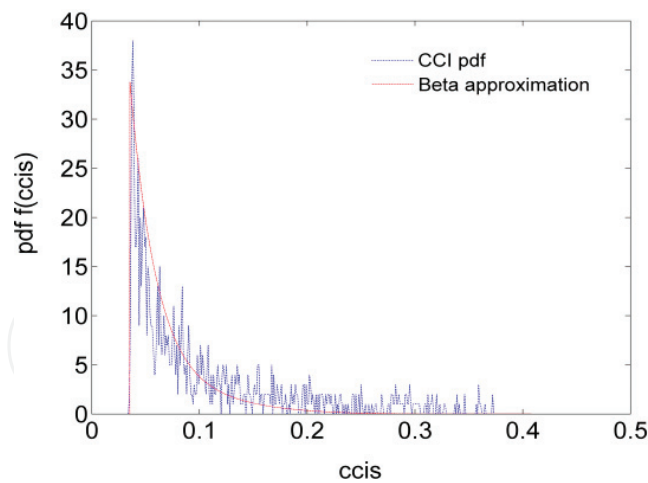


Figure 5. Beta collective approximation of CCI distribution in use case two.

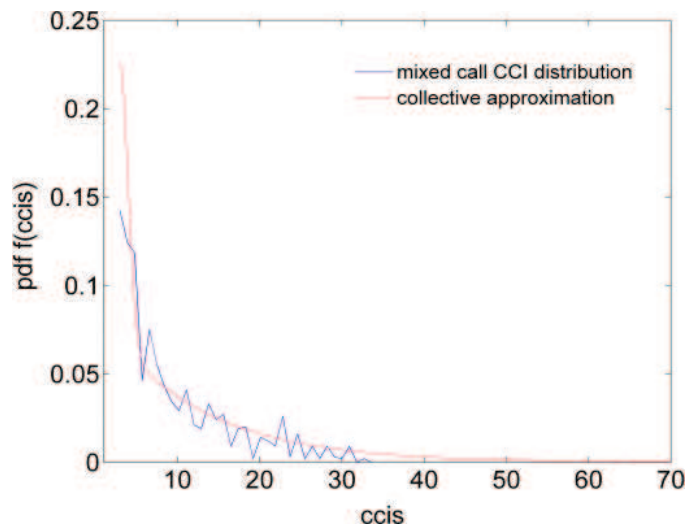


Figure 6. Combined exponential and normal collective representation of mixed call CCIs.

Both use cases in **Figures 5** and **6** illustrate the averaged total CCI power temporal variation when the equally probable random short calls at the co-color user reverse channels progress at full system load. A more realistic scenario of use case two is that the user short call holding times also vary randomly. This scenario can be modeled by weighting the 1000 user call times by a random number generator for each co-color beam which also embodies the spatial CCI variation of that beam. A simple CCI spatial variation approximation has been made in use case one [10]. Clearly, depending on the intended SNIR distribution estimation, the total nominal CCI power variation represented collectively by the random variable τ_0 in Eq. (3b) can be modeled in a variety of ways.

6. Sample applications

In this section, we assess Ka-band HTS system user reverse channel SNIR performances in use cases defined above and present the sample assessment results using the model system of **Figures 2** and **3** and the assumptions made progressively in Sections 3 through 5. They serve to capture the typical geostationary Ka-band HTS system characteristics essential in system design. We also show the wide range applicability and scenario representation flexibility of the models. A central signal green reuse 3 system (CSBg3) is defined with the signal beam being at the center of the service coverage area at the intersection of the fifth column and third row of the green reuse beams in **Figure 2** similar to ESBg3. We exam:

- Use case two CCI distributions characteristics and comparison
- Traffic distribution and user location impact on the SNIR distribution by use case one
- Beam average SNIR distributions and comparison for use case two
- Individual short call SNIR pdfs in all short call scenario of use case two
- Steady call SNIR distributions in a mixed call environment of use case three

The green reuse beam system of **Figure 2** is simulated as shown in **Figure 7** for use. The light green beam shows the ESB whereas the CSB sits in the middle among the five dark green beams. They are used with user case two and three results presented below. Gaussian user location distribution is used for **Figure 7** whereas both Gaussian and uniform user location distribution are used for SNIR performance evaluation. We choose the centers of the user location distributions at the co-color beam centers. The beam centers are determined according to the service demand of the area. For user case one, the simplified user random location scheme presents one user per co-color beam within the beam coverage area [10].

Continuing on CCIs, we find that the CCI of CSBg3 is heavier than that of ESBg3 in **Figure 8** and the typical co-color beam CCI spiky distributions in **Figure 9** for use case two. Clearly, the

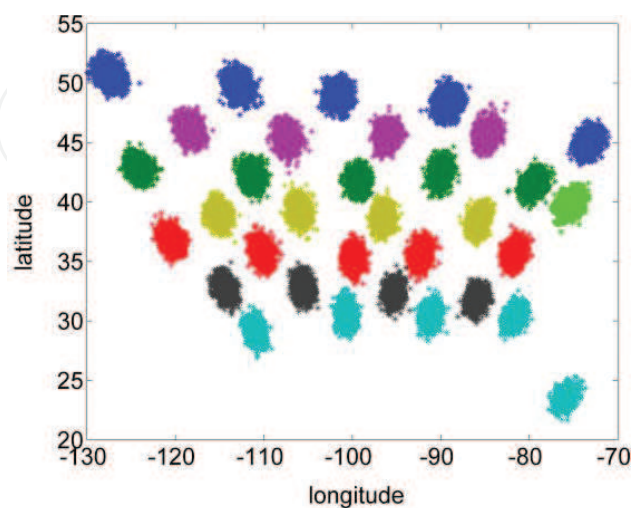


Figure 7. ESBg3 Gaussian co-color beams simulation illustration.

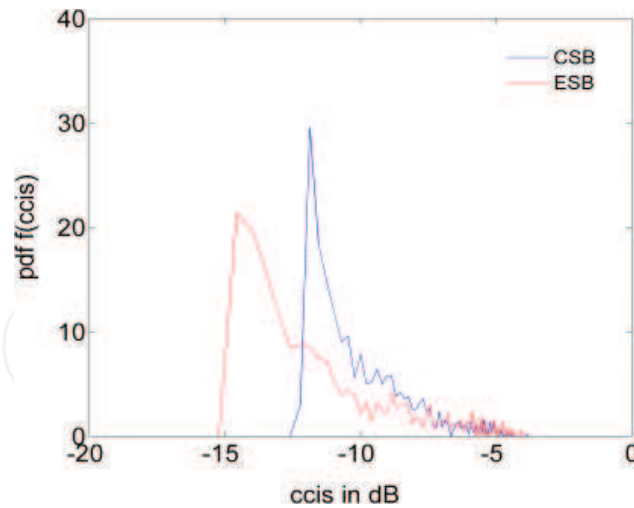


Figure 8. Total CCI distribution comparison.

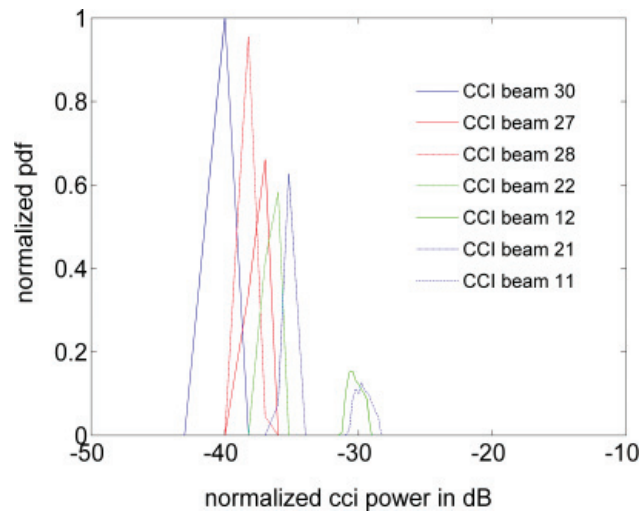


Figure 9. Individual beam CCI distribution.

average 2.5 dB more CSBg3 CCI results because the CSB is surrounded four sides by the close-by first 2 tier CCIs whereas the ESB faces them in three sides only. The individual beam CCI distributions are shaped like spikes within 3 dB because of the many non-linear transformations from the user location Uniform distribution in contrast to the signal beam power distribution which approximates a Uniform.

The traffic distribution impact and typical co-color beam user location random variation effects on ESBg3 user reverse channel SNIR performance for use case one are shown in **Figures 10** and **11**. The traffic distribution in **Figure 4** is used for **Figure 10** which results in up to 1 dB difference at peaks. This is because in use case one, the CCI gain reduction with Gaussian satellite antenna radiation pattern is much more pronounced than traffic load variation in the system. **Figure 11** further shows that the simplified CCI user random location in use case one renders SNIR distribution approximately 1 dB that of all co-color users at the beam centers.

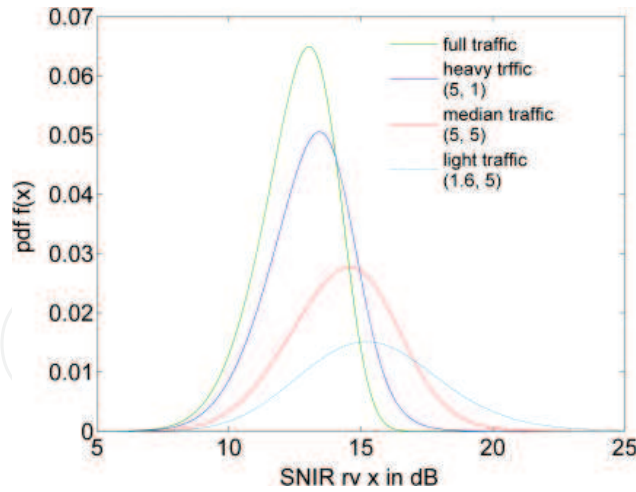


Figure 10. Traffic impact (CSBr4).

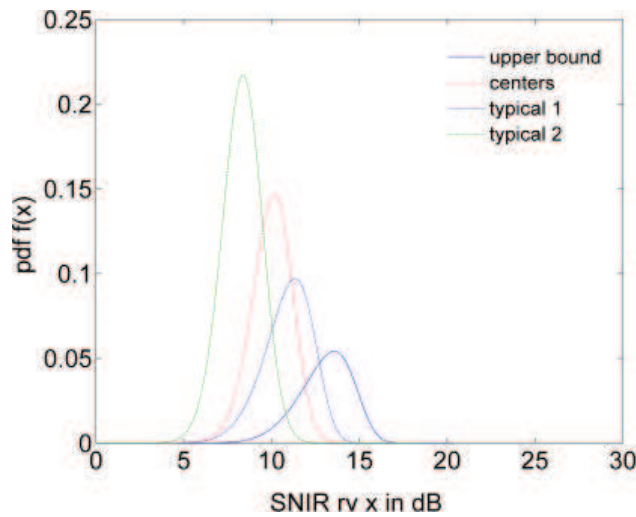


Figure 11. ESBg3 user location effect.

Therefore, the all center user SNIR distribution is a fair approximation of the beam SNIR distribution average [10].

For use case two of all short calls Uniform or Gaussian distributed in each and every co-color beams, only the beam average signal-to-interference ratio (SIR) or SNIR using average noise power spectrum density is measurable and meaningful. In **Figures 12–14**, we compare the beam average SNIR distributions in CS LOS channel conditions with fixed channel power loss:

$$f_{SNIR} = f \left(\sum_{j=1}^{1000} \frac{S(x_j, y_j)}{n_0 + \sum_{k=1}^{32} I_k(x_{j,k}, y_{j,k})} \right) \tag{17}$$

where f denotes the frequency counts of the SNIR values calculated at 1000 users in the parenthesis.

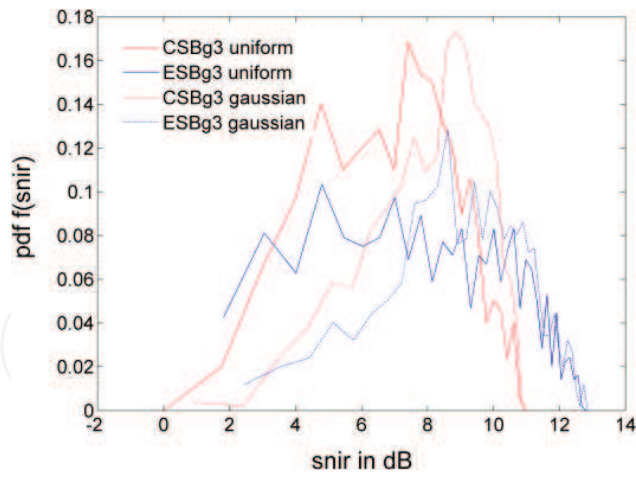


Figure 12. A beam average SNIR distribution comparison.

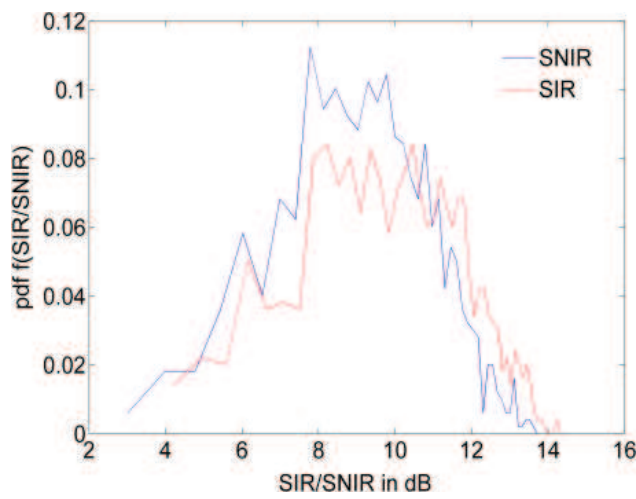


Figure 13. Beam average SIR/SNIR.

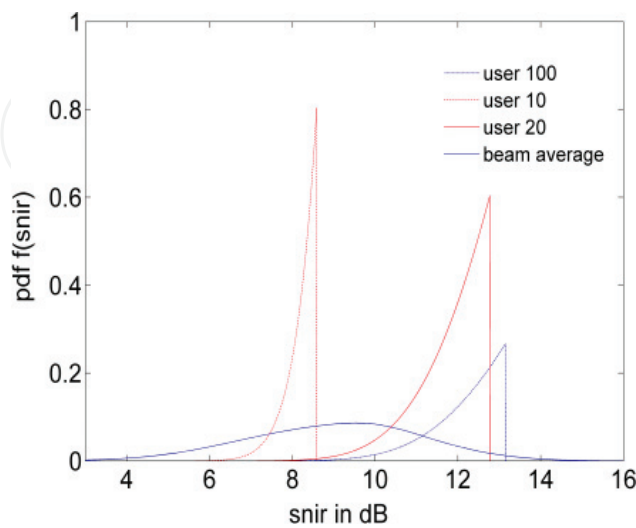


Figure 14. Individual user SNIRs.

Among the four distributions in **Figure 12**, the user location Uniform distributed SNIR pdfs show a flat top from 4 dB to approximately 9 dB whereas the user location Gaussian distributed SNIR pdfs are pointed with peaks at approximately 8 and 9 dB. This results because the Gaussian user location distribution produces higher user density at the beam center but much lower density of users at the edge of the beam coverage area compared to Uniform user location distribution in which users are evenly distributed in the beam coverage area. The former has a larger distance separation between CCI users and signal users which results in less CCIs as shown in **Figure 8**. Consequently, the SNIR performance improves. **Figure 12** also shows the ESBg3 system performs 2 dBs better on the high end due to the overall less first 2 tier CCIs. The high pdf value at low CCI power results because the many more low CCI powers produced by the many far away CCI beams exit in the ESBg3 system. **Figure 13** plots the average beam performance degradation by approximately 2 dB at the high end and 1 dB average at the low end because of the inclusion of noise.

The beam average SNIR power spreads are approximately 11 dB in **Figure 12** with ESBg3 leading 2 dB higher at high end. When noise is taken as a fixed power density value, the individual user SNIR is a fixed value for short reverse channel calls. If the noise power is taken as a random variable instead of the mean power density for individual users and by treating the CCI power as a delta function as shown in Eq. (7), we find the SNIR distributions for the typical user short calls of user case two in **Figure 14**. Clearly, for short calls where the signal and the CCI are assumed fixed power levels, the SNIR starts from a fixed value and spreads to the lower end to left as noise power spreads to the higher end at right. Compared to the beam average SNIR spread of approximately 11 dB also shown in **Figure 14**, the individual call SNIRs vary only 2–3 dB.

By treating the total CCI as a fixed value and using delta function as its pdf representation as shown in Eq. (7), we reach the beam average SNIR via probability theory using Eqs. (4–5).

Figure 15 shows the good approximation of the beam average SNIR distribution of the user Gaussian distributed ESBg3 system by applying the probability models. The high end

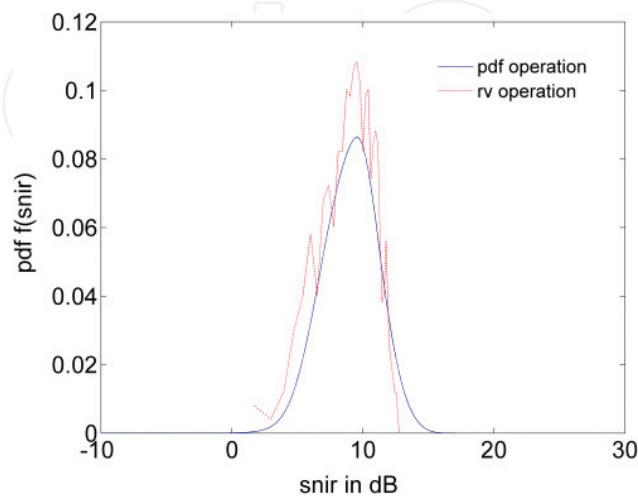


Figure 15. ESBg3 beam average SNIR distribution.

mismatch is due to the large noise power spread of the noise probability model used with pdf operation. The beam signals for the figure are approximated by a Beta distribution collectively. The parameters of the figures are given in **Table 2** in the Appendix A.

For use case three of mixed calls, we set three CCI beams holding the long call with ESB. They are the beams at Caribbean, in the middle of the continent US and at the northwest of the continental US. The rest of the CCI calls are short random calls one at a time in a beam. The ESB is located at the northeast of continental US by the edge of the service area. The total 29 short CCI calls vary a little from that of the 32 short calls in distribution. The short call CCI distributions are collectively modeled as a weighted combination of exponential and Gaussian in Eq. (16) whereas the long signal and CCI calls are each χ^2 distributed with a power scaling factor determined by the satellite antenna radiation pattern angular filtering. As shown in **Figure 16** the SNIR performance of user Gaussian distributed ESBg3 outperforms the user Uniform distributed ESBg3 SNIR by approximately 4 dB at peak and Gaussian SNIR is approximately equally probable from 6 to 12 dB indicating a consistent performance at the power spread range. Compared to the user location Uniform distributed mixed call ESBg3 SNIR, it ceases approximately 2 dB higher in power spread at lower end because of the low density CCI users at the beam edges.

Compared to the beam average SNIR performance of use case two with all short reverse channel calls shown in **Figures 12** and **15**, the SNIR of use case three mixed calls of **Figure 16** shares with them the most probable power level of about 10 dB at Gaussian user location distribution. They differ however in spreads for about 2–4 dB because, in part, that the long call χ^2 distributions and the noise exponential distribution included in **Figure 12** contribute to the larger SNIR power spread than that of the beam average SNIRs. Compared to the user case one of **Figures 10** and **11** for which the Gaussian satellite antenna radiation pattern is used, use case two and three is less performing in SNIR power level because the sharp slope of the Gaussian antenna pattern filters out much more CCI power. In those simplified random individual user location scenario, the channel SNIRs are approximately 10 dB less in spread due to the CCI power spatial simplification.

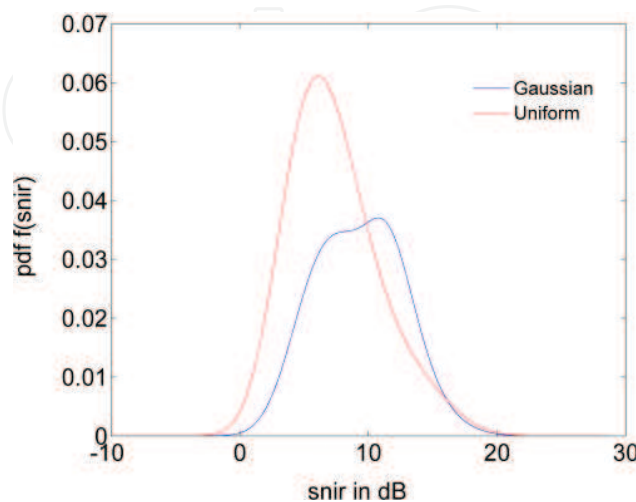


Figure 16. ESBg3 mixed call SNIR distributions.

7. Conclusions

Two approaches are commonly used in assessment of a complex system of many variables including random variables. They are simulation and analytical approaches or a combination of the two. Ka-band HTS systems are complex systems with many uncertain quantities including traffic loads, channel weather conditions, and intra-system CCIs. This study chooses the random variables of the system of statistical significance, and develops the probability models by taking an analytical approach to characterize the variations of the system or channel SNIRs, the most important QoS measure of a Ka-band HTS system. It results in a closed analytical SNIR distribution model which can be implemented by numerical evaluations, leading to significant savings in both computation time and storage. Complementary to the known studies [4–8], it captures the statistics of the random variations relevant to SNIR estimation by abstraction and fills in the blank of the study of the topic for urban and mobile user scenarios.

By treating the signal and CCI power variation caused by the channel conditions as random variables and the traffic variation and CCI power variation caused by satellite antenna radiation pattern angular filtering with collective representations, this study allows for system offered user uplink SNIR prediction with significantly reduced computational complexity in the early stage of a system design. It is statistically accurate for user uplink SNIR estimation in multi-path channel environments particularly [10].

Our discussion of the model application focuses on the collective representation of application scenarios in CS LOS channel conditions in this chapter. The sample application result of **Figure 9** confirms the beam CCI distribution reported in [4–6]. Moreover, it can be inferred by an examination of **Figures 5, 6, 8** that the total CCI distribution can verify the half Gaussian distribution assumption made in [8] if less mid-range CCIs more far away tier CCIs are filtered into the satellite receiver by the satellite antenna radiation pattern. The average beam CCI power distribution spread of 14 dB is comparable to the 15 dB found in [4–6]. The 1 dB difference should come from the different number of beams which is 43 in ESA's system performance simulation whereas it is 101 in this study. Though not shown here, our other sample results with ESBg3 and CSBg3 share the spatial CCI distribution characteristics with those reported in ESA.

Compared to ESA study of the same topic, the collective representation of this study can achieve the same traffic simulation effects by profiling the user traffic factor in Eq. (3b) and therefore predict the system capacity performance at offered SNIR distributions for a wide range of system architecture and operational scenarios. However, it can't achieve the interactive design of the physical layer of the system for optimal resource allocation at different system traffic loads by the total system simulation efforts reported in [4–6, 8]. It can be used in the initial stage system architecture design and performance prediction at beam and user level stand alone or incorporated into total system operation simulation packages as a SNIR estimation unit. In real system design, user population probability models and beam centers can vary in accordance with the service area and population distribution. The study is applicable to real system satellite and user antenna radiation patterns and other system parameters. The sample results should improve with them [4–6, 10].

A. Appendix A

Figure 5: use case two of ESBg3 short calls with user location Uniformly distributed

Semi-minor uniform $(-164, 164)$; semi-major uniform $(-185, 185)$

$a_1 = 0.6, b_1 = 0.4, \alpha_1 = 1, \alpha_2 = 1, \beta_1 = 17, \beta_2 = 6, \max(\text{ATT}_{\text{ccisum}}) = 0.3898$

Figure 6: use case three of ESBg3 mixed calls with user location Gaussian distributed

Semi-minor Gaussian $(0, 53)$; semi-major Gaussian $(0, 75)$

$a_2 = 0.55, b_2 = 0.45, \lambda = 9, \mu = 5, \sigma = 2.5$

Table 1. User total CCI collective representation parameters at $\theta_{3dB} = 0.5^\circ$ and $\lambda_S = -99^\circ$.

Figures 14 and 15: use case two at short calls of user location Gaussian distributed

Semi-minor Gaussian $(0, 53)$; semi-major Gaussian $(0, 75)$;

Signal: $\text{beta}(6, 1)$; Noise: $n_0 = 0.0134$; CCI: **Figure 6** parameters;

Figure 16: use case three of mixed calls

Steady call¹ CCI beam numbers: 5, 16, 25, 32; χ^2 distribution K factor: 100

¹The four calls that last the entire SNIR evaluation time frame when the other calls are short bursts in the mixed call use case three

Table 2. ESBg3 SNIR distribution parameters at $\theta_{3dB} = 0.5^\circ$ and $\lambda_S = -99^\circ$.

Author details

Liping Ai* and Hermann J. Helgert

*Address all correspondence to: lai002@gwu.edu

George Washington University, Washington, DC, USA

References

- [1] Fenech H. What pushed us into HTS systems? In: 23rd Ka and Broadband Communications Conference and 35th AIAA ICSSC; Trieste, Italy; 16 October, 2017
- [2] Mclain C et al. Future Ku-band mobility satellites. In: 23rd Ka and Broadband Communications Conference and 35th AIAA ICSSC; Trieste, Italy; 17-October-2017
- [3] Ippolito L. Satellite Communications Systems Engineering. 2nd ed. Wiley; 2008. ISBN-13: 9780470725276

- [4] Schweikert R et al. ESA STUDY CONTRACT REPORT: Protocols and Signaling for Adaptive Fade Mitigation Techniques (FMT) in DVB-RCS Multi-Beam Systems, Final Report. European Space Agency (ESA); AUDENS ACT 2005
- [5] Schweikert R et al. Protocols and Signaling for Adaptive Fade Mitigation Techniques (FMT) in DVB-RCS Multi-Beam Systems, Technical Report 1: Scenario Definition and Benchmark Assessment. ESA Reports; 2005
- [6] Gallinaro G et al. Adaptive Coding Modulation Techniques for Ka/Q Band Systems – TN1 Reference Scenario Definition. European Space Agency (ESA); 2003
- [7] Fenech H. High throughput satellite systems: An analytical approach. IEEE Transactions on Aerospace and Electronic Systems. 2015;51:192-202
- [8] Rinaldo R et al. Capacity analysis and system optimization for the reverse link of multi-beam satellite broadband systems exploiting adaptive coding and modulation. International Journal of Satellite Communications and Networking (IJSCN). 2004;22:425-448
- [9] ITU-R. Satellite antenna radiation pattern for use as a design objective in the fixed-satellite service employing geostationary satellites. ITU-R S.672-4; 1997
- [10] Ai L. A Novel Study of the SNIR distributions of Ka-band HTS systems [PhD dissertation]. George Washington University; 2016
- [11] Wakana H et al. Fade characteristics for K-band land-mobile satellite channels in Tokyo measured using COMETS. Electronics Letters. 1999;35(22):1912-1913
- [12] Leon-Garcia. Probability, Statistics and Random Processes for Electrical Engineering. Upper Saddle River: Pearson Education; 2008. p. 07458
- [13] ITU-R. Propagation Data and Prediction Methods Required for the Design of Earth-Space Telecommunication Systems. ITU-Recommendation on Propagation.618; September 2013